J Mater Sci (2007) 42:6755–6761
DOI 10.1007/s10853-006-1465-x

Absorption and emission spectral analysis of Pr^{3+}: tellurite glasses

K. Annapurna · Ritwika Chakrabarti · S. Buddhudu

Received: 20 July 2006 / Accepted: 15 December 2006 / Published online: 27 April 2007

Abstract This paper reports on the results concerning optical absorption and fluorescence properties of $60TeO_2$–$25ZnO$–$10BaO$–$4.5La_2O_3$–$0.5Pr_2O_3$ (Pr^{3+}: TZBL) glass. Both electronic (α_e) and vibrational (α_v) band edge cut-off wavelengths of the host glass (TZBL) have been evaluated from the measurement of its UV–Vis and IR transmission spectra. The glass studied has shown 80% transmittance throughout its optical window from 0.366 μm (α_e = 3.39 eV) to 6.30 μm (α_v = 0.197 eV). The FT-IR transmission spectra of Pr^{3+} doped and also reference tellurite glasses have demonstrated the presence of TeO_4 and TeO_{3+1} or TeO_3 structural units. The thermal properties of this glass have been investigated from the study of DTA profile. The recorded optical absorption spectra of Pr^{3+}: TZBL glass have shown eight absorption bands from 300 nm to 2,500 nm. The fluorescence emission has been observed mainly from $^3P_1$, $^3P_0$ and $^1D_2$ states to the lower lying states and which are assigned to the transitions of $^3P_0 \rightarrow {}^3H_{4,5,6}$; $^3P_0 \rightarrow {}^3F_{2,3,4}$; $^3P_1 \rightarrow {}^3H_5$ & $^1D_2 \rightarrow {}^3H_{4,5}$ upon excitations at three excitation states of $^3P_{0,1,2}$. From the time resolved spectra, it is found that $^3P_0$ level decays faster than $^1D_2$ level. The fluorescence decay kinetics of $^3P_0$ and $^1D_2$ levels have been measured and the lifetimes are found to be 21 and 39 μs, respectively.

K. Annapurna (✉) · R. Chakrabarti
Glass Technology Laboratory, Central Glass & Ceramic Research Institute, Kolkata 700 032, India
e-mail: glasslab42@hotmail.com

S. Buddhudu
Department of Physics, Sri Venkateswara University, Tirupati 517 502, India

Introduction

Trivalent rare earth ions doped glasses have been identified as very important class of materials as fluorescent display devices, optical detectors, bulk lasers, fiber amplifiers and waveguide lasers [1–3]. In order to update the glass science and technology, several new optical systems are being brought out from different laboratories in the world from time to time. We are all aware of the fact that the materials with low phonon energies are preferable and such optical systems could significantly encourage in obtaining better and potential emission performance from the dopant luminescent rare earth ions. But, some of the low phonon energy glass hosts such as halide glasses could possess poor chemical durability and chalcogenide glasses essentially require more stringent preparation conditions compared to the oxide glasses. Hence, recently heavy metal oxide (HMO) glasses have been found to be more promising glassy materials for photonic applications with reasonably low phonon energies [4, 5]. Among the HMO glasses, tellurite glasses are more attractive systems with advantages such as low temperature of melting, good corrosion resistance, better thermal stability, low phonon energy, wide transmission region (0.36 μm–6.3 μm), high refractive index and desired rare earth concentration in the matrices [6]. In recent years, tellurite based glasses have extensively been investigated towards the development of fiber amplifiers for use in broadband telecommunication applications [7]. Due to their high refractive index and the presence of lone pair of electrons in electronic structure, those could be functioning as good candidates in the development of certain nonlinear optical devices like optical switches with a large third order nonlinear susceptibility. Thermally poled tellurite based glasses containing zinc or alkaline earth/alkali ions have demonstrated

a second harmonic generation (SHG) [8, 9]. The binary zinc–tellurite glass systems have been studied widely for their structural details as well as their luminescence properties with Pr^{3+} or Nd^{3+} as the dopant ions due to their technological advantages [10]. Chen et al., have earlier investigated the Er^{3+} doped TeO_2–BaO (Na_2O/Li_2O)–La_2O_3 glass for its thermal and spectral properties [11]. It has been reported that, the glass without the alkali has shown a good glass thermal stability and with the inclusion of an alkali in the network stability decreases. Hence, barium-containing glasses are considered as good candidates for optical materials, as it improves the glass stability, chemical resistance, optical refractive index and also it reduces the phonon energy to a certain extant. There has not so far been any information on zinc–barium–tellurite glass system. Earlier, we have reported on the energy transfer mechanisms in the rare earth pairs such as (Eu^{3+}, Nd^{3+}) and (Dy^{3+}, Nd^{3+}) doped in tellurite glasses [12, 13]. In the present work, our main objective is to study the spectral properties of Pr^{3+}:TeO_2–ZnO–BaO–La_2O_3 (TZBL) glass system. Among the rare earth ions, Pr^{3+} has been widely used because of its emission at 1.3 μm so called second telecom window [14]. Apart from this, Pr^{3+} ions have the ability to show four level laser action associated with transitions from $^3P_0$ state in certain host systems as the potentially active ions for a visible laser generation [15]. The present paper brings out the results pertaining to the studies carried out on different physical, thermal and optical absorption and emission spectra of Pr^{3+} doped TeO_2–ZnO–BaO–La_2O_3 (Pr^{3+}: TZBL) glass.

Experimental studies

Pr^{3+} ions doped tellurite glasses in the composition of $60TeO_2$–$25ZnO_2$–$10BaO_2$–$4.5La_2O_3$–$0.5Pr_2O_3$ have been prepared by means of conventional quenching and annealing methods. The raw materials such as TeO_2 (99.99%) from Alfa, $BaCO_3$ (99.98%) from EMerck, ZnO (99.95%) from Fluka, La_2O_3 (99.98%) from IREL and Pr_4O_{13} (99.99%) from Alfa have been used in the glass preparation. Appropriate amounts of chemicals for 15 gm batch were weighed, mixed thoroughly in the Agate mortar and those chemicals mixtures were melted in pure Platinum crucible with lid at 950 °C for half an hour in a microprocessor controlled electric furnace. A reference glass (without the dopant Pr^{3+} ions) was also prepared under the similar conditions. The prepared samples were annealed at 350 °C temperature for an hour. The densities (d) of the glass samples were measured by following the traditional Archimedes' principle with water as an immersion liquid. The refractive indices at different wavelengths for the reference glass (TZBL) were measured on a precision spectrometer (Kalnew, Model GMR-1) by adopting a minimum deviation method. The XRD analysis of annealed TZBL reference glass and Pr^{3+}: TZBL glass were done on a X-ray diffractometer type PW710 with Cu K_α radiation (1.54Å) in the 2θ range of 10–60 with 0.5 s per step. FT-IR transmission spectra of both the glasses in the range 2,000–400 cm^{-1} were measured using KBr pellet method on a Perkin-Elmer FTIR spectrophotometer model 1615 series with 4 cm^{-1} resolution. The transmission spectra of TZBL glass sample in the range 200–1,100 nm were measured on Perkin-Elmer UV–Vis spectrophotometer model Lambda 20 and in the spectral range 5,000–1,000 cm^{-1} on Perkin-Elmer FTIR spectrophotometer model 1615 series. The UV–Vis–NIR absorption spectra of Pr^{3+}: TZBL glass were recorded on a Perkin-Elmer UV–Vis spectrophotometer model Lambda 20 in the wavelength range of 200–1,100 nm and on Shimadzu MPC3103 UV–Vis–NIR spectrophotometer from 1,000 nm to 2,500 nm. The study state emission spectra and also excitation spectra were recorded on a SPEX Fluorolog-2 spectrofluorimeter with 150 W Xenon lamp as the source of excitation. The time resolved fluorescence spectra and emission transition decay kinetics were measured on the same instrument equipped with 1934D phosphorimeter attachment alongwith a 50 W pulsed xenon lamp as the pump source. The system employs Datamax software in acquiring the spectra and the decay curves.

Results and discussion

Amorphous natures of the Pr^{3+} doped and undoped TZBL glasses have been verified from the X-ray diffraction analysis. Figure 1 shows the DTA curves of Pr^{3+} doped and

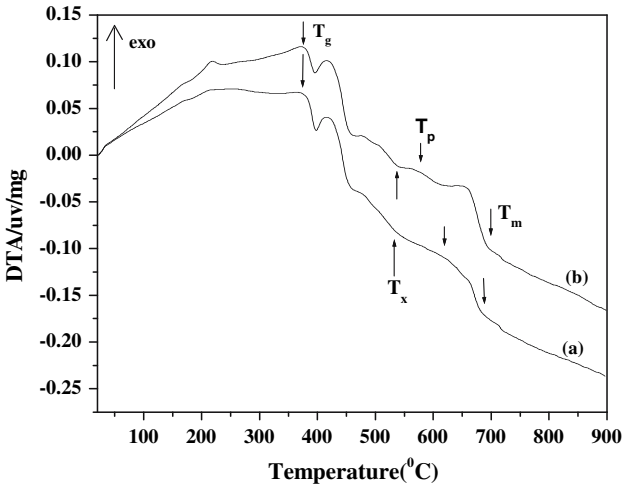

Fig. 1 Differential thermal analysis curves of (**a**) TZBL and (**b**) Pr^{3+}: TZBL glasses

undoped TZBL glasses. The glass transition temperatures (T_g) have been determined to be 380 °C for TZBL glass and 379 °C for Pr^{3+}: TZBL glass. Hence the substitution of lanthanum for Praseodymium in the network is decreasing the glass transition temperature, which is palpable due to the smaller radius of the dopant ion. The DTA curves of both the glasses exhibit no prominent exotherm peak but there is broad hump with insignificant height is seen in the figure suggesting the slow rate of crystallization of these glasses at temperatures near T_x. The thermal stabilities of the TZBL reference glass and Pr^{3+}: TZBL glass have been evaluated from their glass transition temperature (T_g), crystalization onset temperature (T_x) and the melting temperature (T_m) values and the results are listed out in Tables 1 and 2, respectively. The glass stability factor (STF = T_x–T_g) for this glass system is comparable to the first commercially available which is reported to be most stable telluride glass fiber of composition (TeO_2–ZnO–Na_2O) [16]. From the measured density (d) and refractive indices (n), many other important physical, optical and nonlinear optical properties have been estimated using standard expressions and the results are presented in Table 1 for the TZBL glass and in Table 2 for the Pr^{3+}:

Table 1 Different physical, optical and thermal properties of TZBL (reference) glass

Parameters	Data
Physical and optical properties	
Molecular weight of glass (M g)	147.73
Density (d g cm^{-3})	5.452
Refractive index (n)	
$n_{f'}$	2.0629
n_e	2.0369
$n_{c'}$	2.0135
Electronic band edge energy (α_e eV)	3.39
Vibrational band edge energy (α_v eV)	0.197
Reflection losses (R%)	11.658
Molar refractivity (R_M cm^3)	13.88
Molecular electronic polarisability (α_e $Å^3$)	5.5
Mean dispersion ($n_{f'}$–$n_{c'}$)	0.0494
Abbe number (υ_e)	20.9899
Non-linear refractive index ($n_2 \times 10^{13}$esu)	21.915
Non-linear refractive index coefficient ($\gamma \times 10^{-18}$ cm^2/W)	4.51
Nonlinear susceptibility ($\chi^3{}_{1111} \times 10^{15}$)	1.184
Thermal properties	
Glass transition temperature (T_g °C)	380
Crystallization initiation temperature (T_x °C)	532
Crystallization peak temperature (T_P °C)	619
Melting temperature (T_m °C)	680
Glass stability factor (T_x–T_g)	157
Hurby value ($H = (T_x–T_g)/(T_m–T_P)$)	2.5

TZBL glass. It is well known that, the high refractive index glasses have faster responding nonlinearties over the other organic or semiconducting nonlinear materials and for these materials, the nonlinear coefficient is an important property. Tellurite glasses are such systems widely used for fast optical switches [17]. From Table 1 it is found that the TZBL glass possesses high nonlinear refractive index (n_2) and nonlinear coefficient (γ) and hence which demonstrate its suitability for their use in nonlinear optical device applications.

The structure of TeO_2 rich glasses contains basically of three dimensional network of TeO_4 trigonal bipiramidal (tpb) units having two each of oxygens at two equatorial and axial sites with one other equatorial site being occupied by a lone pair of electrons. On the introduction of a modifier, three dimensional network breaks down with the transformation of TeO_4 units into TeO_{3+1} and TeO_3 units [18]. In order to have an insight into the structural units of glasses studied, FT-IR transmission spectra of TZBL and Pr^{3+}: TZBL glasses have been recorded in the range 1,000–375 cm^{-1} as shown in Fig. 2. The spectra have displayed three bands at 758, 677 and 424 cm^{-1} and are assigned to stretching vibrations of TeO_3 or TeO_{3+1}, TeO_4 structural units and bending vibrations of Te–O–Te or O–Te–O linkages respectively following the literature reports [19]. According to them, the ratio of 780/675 cm^{-1} represents the relative concentrations of the TeO_3 and TeO_4 structural units, which is absolutely dependent on the glass composition. From the FT-IR spectra of both glasses, the absence of IR vibrational peaks at 800–780 cm^{-1} indicates that there are no isolated TeO_3 structural unit in the glass composition studied. Also a highest phonon band at 758 cm^{-1} has appeared as a shoulder to the main peak at 677 cm^{-1} which is otherwise found in dominant intensity in some tellurite glass systems of compositions having different other modifiers with almost equivalent molar fractions considered in the present glass composition was explained due to the formation of TeO_3/TeO_{3+1} pyramids with non-bridging oxygens (NBOs) [19]. The intensity dominance of vibrational band at 677 cm^{-1} over the band at 758 cm^{-1} detected in the present glass system could be attributed to be due to the incorporation of ZnO as glass former into a chain like structure with Te_3O_8 groups built by TeO_4 and two TeO_{3+1} units connected by six coordinated Zn^{2+} ions [20] and the contribution of stretching vibrations due to Zn–O bond are also expected at this wavenumber. The peak at 758 cm^{-1} as a shoulder to the main peak at 677 cm^{-1} could be resulted due to the superposition of TeO_{3+1} and TeO_3 units, which have formed by the distortion of TeO_4 units in the presence of BaO and La_2O_3 as modifiers. This assortment of species in the tellurite glass matrix indicates the presence of a variety of structural sites due to the incorporation of modifiers.

Table 2 Different physical and thermal properties of Pr^{3+}: TZBL glass

Characteristic parameters	Data
Physical properties	
Molecular weight of glass (M g)	147.75
Density (d g cm^{-3})	5.442
Rare earth ion concentration ($N \times 10^{21}$ ions cm^{-3})	1.1092
Ionic radius (r_p Å)	3.893
Inter ionic distance (r_i Å)	9.660
Field strength ($F \times 10^{-15}$ cm^2)	1.979
Thermal properties	
Glass transition temperature (T_g °C)	379
Crystallization initiation temperature (T_x °C)	539
Crystallization peak temperature (T_P °C)	575
Melting temperature (T_m °C)	694
Glass stability factor (T_x–T_g)	160
Hurby value ($H = (T_x–T_g)/(T_m–T_P)$)	1.3

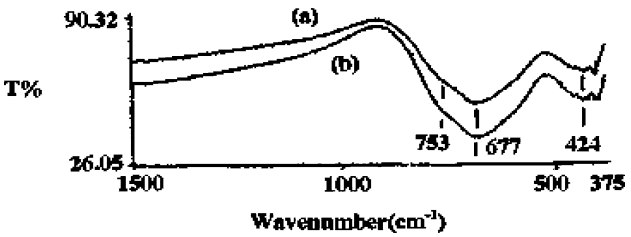

Fig. 2 FT-IR transmission spectra of (**a**) TZBL and (**b**) Pr^{3+}: TZBL glass

Figure 3a, b shows the transmission characteristics of a reference glass (TZBL glass) in the UV–Vis–NIR range. From these transmission curves, electronic (α_e) and vibrational (α_v) absorption edge wavelengths have been estimated as shown in Fig. 3a, b and the results are given in Table 1. It is clear from this figure that, the TZBL glass has above 80% transmission in the entire range of optical window between 0.366 μm and 6.30 μm. The vibrational absorption edge at 6.30 μm (1,587 cm^{-1}) in the IR transmission spectrum of TZBL glass has been resulted from the overtones of the Te–O stretching vibrations at 800–600 cm^{-1} as noticed in its recorded FTIR spectrum. The absorption peaks detected in IR transmission curve at 3.2 μm (3,128 cm^{-1}) and 4.4 μm (2,328 cm^{-1}) are due to stretching vibrations of hydroxyl (OH^-) groups. Earlier in the literature, many tellurite glasses exhibited vibrational bands due to OH^- groups in the range 2,300–3,500 cm^{-1} and they were assigned to be as follows: the band at ~3,500 cm^{-1} is due to hydrogen bond free OH^- groups, the band at ~3,000 cm^{-1} is due to weak hydrogen bonding between NBO and OH^- groups and the band at ~2,500 cm^{-1} is due to the strong hydrogen bonding of OH^- to NBO [21, 22]. Accordingly, in the present glass, the observed bands at 3,128 and 2,328 cm^{-1} are considered due to weakly and strongly hydrogen bonded OH^- groups, respectively. And it can be stated that, the hydrogen bond free OH^- groups are absent as there is no band observed at around 3,500 cm^{-1}. In the rare earth doped glasses, OH^- group act as fluorescence quenching sites, which promote non-radiative decay of emitting level and ultimately decreasing the emission efficiency of the material. More is the absorption coefficient of OH^{-1} (α_{OH}^-), higher would be its influence on the fluorescence quenching. The absorption coefficient of OH^- (α_{OH}^-) which is determined based on the application of a standard procedure made available in literature [23] from the recorded IR transmission spectrum of the glass investigated has been found to be 0.81 cm^{-1} which is certainly a lower value and therefore it could be considered to show a negligible effect on the fluorescence efficiency of the dopant ion in the glass matrix studied here. The recorded optical absorption spectrum of Pr^{3+}: TZBL glass in two wavelength ranges 375–650 nm and 875–2,500 nm are presented in Fig. 4a, b. The glass has revealed eight bands four each in UV–Vis and NIR regions from ground state ($^3H_4$) to various higher energy states of Pr^{3+} ions. They are assigned to the transitions of $^3H_4 \rightarrow {}^3F_2$, $^3F_3$, $^3F_4$, $^1G_4$, $^1D_2$, $^3P_0$, ($^3P_1$, $^1I_6$) and $^3P_2$ depending upon their peak energies. Similarly, the excitation spectrum recorded by monitoring the emission wavelength at 615 nm has been revealed three peaks corresponding to the transitions from ground state to $^3P_0$, ($^3P_1$, $^1I_6$) and $^3P_2$ levels as shown in Fig. 5. The room temperature fluorescence emission spectrum (475–750 nm) of Pr^{3+}: TZBL glass excited by three wavelengths of $^3P_0$, $^3P_2$ and ($^3P_1$, $^1I_6$) bands separately are shown in Fig. 6a, b, c. The emission bands have been labeled as summarized below:

Transition	Wavelength	Color	Significance	Emission type
$^3P_0 \rightarrow {}^3H_4$	(490 nm)	Blue	High	Three level
$^3P_0 \rightarrow {}^3H_5$	(536 nm)	Green	Medium	Four level
$^3P_1 \rightarrow {}^3H_5$	(532 nm)	Green	Medium	Three level
$^1D_2 \rightarrow {}^3H_4$	(604 nm)	Red	High	Three level
$^3P_0 \rightarrow {}^3H_6$	(615 nm)	Red	High	Four level
$^3P_0 \rightarrow {}^3F_2$	(646 nm)	Red	High	Four level
$^1D_2 \rightarrow {}^3H_5$	(688 nm)	Deep red	Low	Four level
$^3P_0 \rightarrow {}^3F_3$	(703 nm)	Deep red	Low	Four level
$^3P_0 \rightarrow {}^3F_4$	(730 nm)	Deep red	Low	Four level

Based on the literature reports, the emission band at 532 nm has been assigned to the transition of $^3P_1 \rightarrow {}^3H_5$, this band has been detected even when its lower laying level $^3P_0$ is excited upon. Thus, it is clear that the emission from $^3P_1$ level is resulting due to its thermal population as

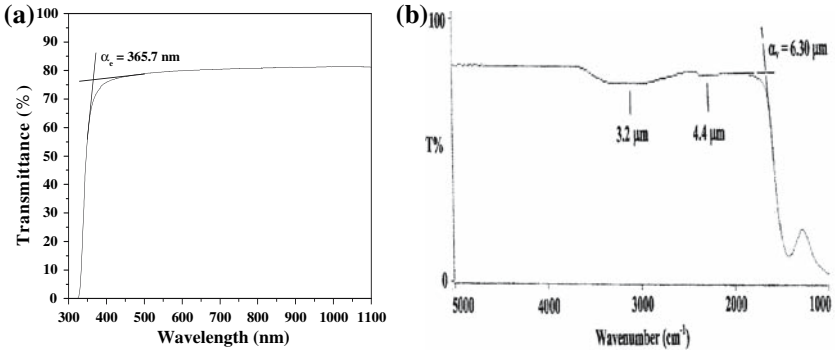

Fig. 3 (**a**) UV–Vis transmission spectra of TZBL glass. (**b**) NIR transmission spectra of TZBL glass TZBL glass

the energy gap between this level and lower laying $^3P_0$ state is only around 650 cm^{-1} [24]. Among the measured emission transitions, $^3P_0 \rightarrow {}^3H_6$ and $^3F_2$ transitions are in the red region and which are more intense. They occur due to the participation of four energy levels, when $^3P_2$ and ($^3P_1$, $^1I_6$) levels are excited which can be seen in partial energy diagram of Pr^{3+}: TZBL glass as depicted in Fig. 7. It is well known that, four level emission is more efficient than three level emission mechanism in the view of practical laser applications. It is observed from the fluorescence spectra that the relative intensities of these two red emission transitions vary with the change in excitation wavelengths. For example, their ratio ($I(^3P_0 \rightarrow {}^3H_6)$/ $I(^3P_0 \rightarrow {}^3F_2)$) are 1.15, 1.03 and 0.89, respectively when excited at 484, 443 and 468 nm, respectively. In the fluorescence spectrum, the intense red emission at 600–630 nm could be due to both $^3P_0 \rightarrow {}^3H_6$ and $^1D_2 \rightarrow {}^3H_4$ transitions with dominant emission from $^3P_0$ level. To verify this, time resolved emission spectra have been carried out for Pr^{3+}: TZBL glass with an excitation at 444 nm ($^3H_4 \rightarrow {}^3P_2$) at varied delay times. The time resolved spectra are shown in Fig. 8a, b, c, d and e. It is noticed from this figure that, with an increase in the time delay from 0.01 ms to 0.1 ms, the emission from $^3P_0$ decreases and at longer delay times, emission from $^1D_2$ level alone could become possible. This provides a good support upon overlay of both the emission transitions $^3P_0 \rightarrow {}^3H_6$ and $^1D_2 \rightarrow {}^3H_4$ in the peak at wavelength 600–630 nm region. This time resolved spectra also used to investigate the time evaluation of the fluorescence from the emitting levels $^3P_0$ and $^1D_2$. It is observed that, $^3P_0$ level decays faster than $^1D_2$ and which has been substantiated from the measured decay curves of emission bands as shown in Fig. 9 and from which lifetimes of the $^3P_0$ and $^1D_2$ emission bands are 21 and 39 μs, respectively.

Conclusions

In summary, it is concluded that we have developed greenish-yellow colored Pr^{3+} doped tellurite glass in the composition of $60TeO_2$–$25ZnO$–$10BaO$–$4.5La_2O_3$–$0.5Pr_2O_3$ and analyzed. Glass thermal properties, FT-IR, optical absorption and time resolved fluorescence spectra have systematically been studied in evaluating the properties of this optical glass. The measured spectrum from UV–Vis to the IR spectra have shown the glass has been transmitting from 365.7 nm (α_e = 3.39 eV) to 6,300 nm (α_v = 0.197 eV) with a 80% transmission within the optical window. The FT-IR transmission spectra of Pr^{3+} doped and also un-doped tellurite glasses have demonstrated the presence of TeO_4 and TeO_{3+1} or TeO_3 structural units. It is believed that, the ZnO presence could be participating in the glass network as six coordinated Zn^{2+} ions. The glass stability factor (GSF) estimated from glass transition (T_g), crystallization onset (T_x), peak (T_P) and melting (T_m)

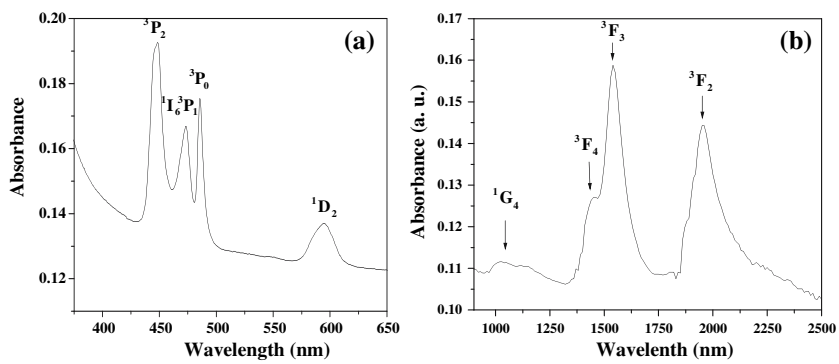

Fig. 4 (**a**) Visible and (**b**) NIR absorption spectra of Pr^{3+}: TZBL glass

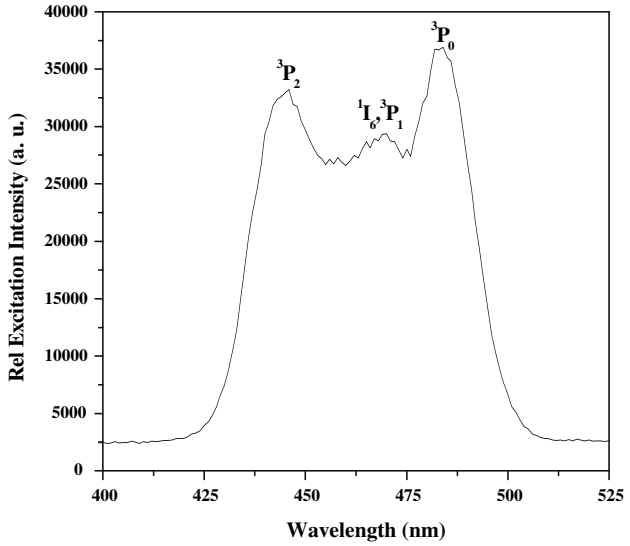

Fig. 5 Excitation spectrum of Pr^{3+}: TZBL glass

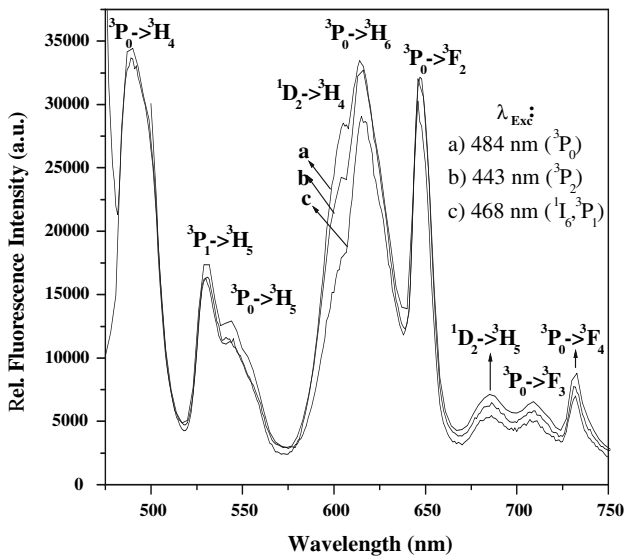

Fig 6: Visible fluorescence spectra of Pr^{3+}: TZBL glass at different excitation wavelengths

obtained from the DTA measurements reveal that the glass examined here possess good thermal stability. Both the measured absorption and emission spectra of the Pr^{3+} glass have been assigned to the appropriate electronic transitions. From the time resolved spectra, it is found that $^3P_0$ level decays faster than $^1D_2$ and at shorter delay times, $^3P_0$ emission dominates while with an increase in delay time, $^1D_2$ emission becomes more effective. The fluorescence lifetimes of $^3P_0$ and $^1D_2$ levels have been computed from the measured decay kinetics and are found to be 21 and 39 μs, respectively. The emission from $^3P_1$ level has been attributed to the thermalization of the closely lying lower state namely $^3P_0$.

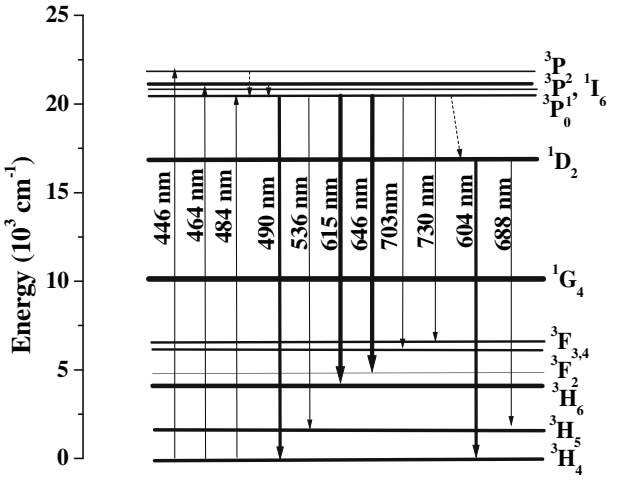

Fig. 7 Partial energy level diagram and emission mechanism in Pr^{3+}: TZBL glass

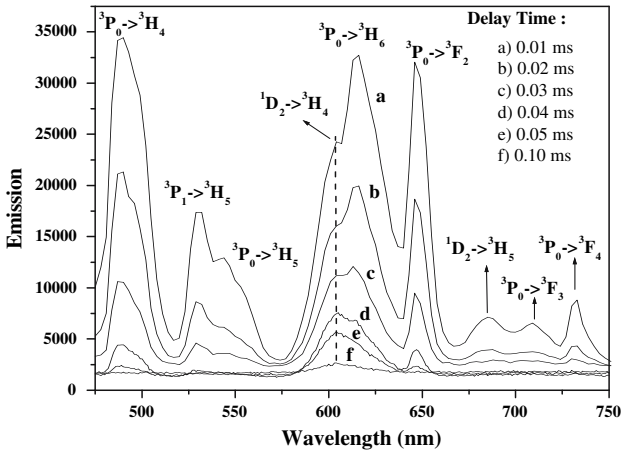

Fig. 8 Time resolved emission spectra of Pr^{3+}: TZBL glass with λ_{exc} = 444 nm

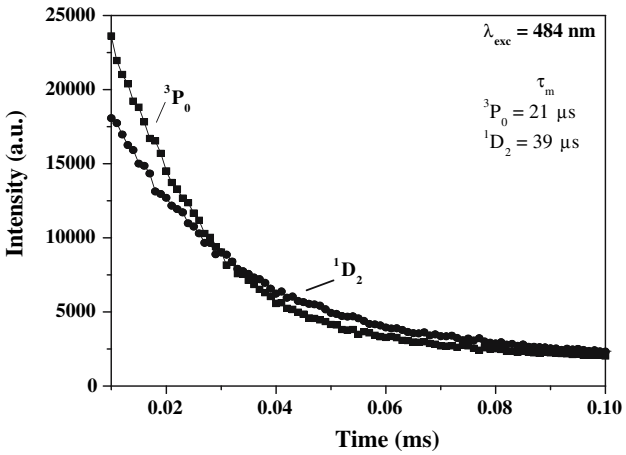

Fig. 9 Fluorescence Decay curves of $^3P_0$ and $^1D_2$ levels of Pr^{3+}: TZBL glass

Acknowledgements Authors would like to thank Dr. H.S. Maiti, Director, CGCRI, Kolkata and Dr. K. Phani, Head, Glass Division, for their kind co-operation and continued support in the present work. One of the authors (RC) expresses her gratefulness to the CGCRI, CSIR for awarding her with a research internship.

References

1. Jackson SD (2003) Appl Phys Lett 83:1316
2. Rakov N, Maciel GS, Sundheimer ML, de S. Menezes L, Gomes ASL, Messaddeq Y, Cassanjes FC, Poirier G, Ribeiro SJL (2002) J Appl Phys 92:6637
3. Lin H, Wang XY, Lin L, Yang DL, Xu TK, Yu JY, Pun EYB (2006) J Lumin 116:139
4. Sun H, Duan Z, Zhou G, Yu C, Liao M, Hu L, Zhang J, Jiang Z (2006) Spectrochim Acta A 63(1):149
5. Pan Z, Morgan SH, Dyer K, Ueda A, Liu H (1996) J Appl Phys 79(12):8906
6. Xu S, Fang D, Jiang Z, Zhang J (2005) J Solid State Chem 178:1817
7. Shen S, Richards B, Jha A (2006) Opt Express 14(12):5050
8. Cacho VDD, Kassab LRP, de Oliveira SL, Morimoto NI (2006) Mater Res 9(1):21
9. Narazaki A, Tanaka K, Hirao K, Soga N (1998) J Appl Phys 83(8):3986
10. Sidebottom DL, Hrushka MA, Potter BG, Brow RK (1997) J Non-Crys Solids 222:282
11. Chen H, Liu YH, Zhou YF, Zhang QY, Jiang ZH (2005) J Non-Cryst Solids 351:3060
12. Annapurna K, Dwivedi RN, Buddhudu S (1999) Mater Lett 40(6):259
13. Annapurna K, Dwivedi RN, Buddhudu S (2000) Opt Mater 13(4):381
14. Bürger H, Kneipp K, Hobert H, Vogel W (1992) J Non-Cryst Solids 151:134
15. Romanowski WR, Sokolska I, Golab S, Lukasiewicz T (1997) Appl Phys Lett 70(6):686
16. Wang S, Vogel EM, Snitzer E (1994) Opt Mater 3:187
17. Takebe H, Fujino S, Morinaga K (1994) J Am Ceram Soc 77:2455
18. Himei Y, Osaka A, Nanba T, Miura Y (1994) J Non-Cryst Solids 177:164
19. Man SQ, Pun EYB, Chung PS (1999) Optics Commun 168:369
20. Fortes L, Santos LF, Goncalves MC, Almeida RM (2006) J Non-Cryst Solids 352:690
21. Krasteva V, Hensley D, Sigel G Jr (1997) J Non-Cryst Solids 222:235
22. Shaltout I, Badr Y (2006) Phys B 381:187
23. Yang JH, Dai SX, Dai NL, Wen L, Hu LL, Jiang ZH (2004) J Lumin 106:9
24. Di Bartolo B, Bowlby BE (2003) J Lumin 102–103:481